# Optical feedback stabilization of photonic microwave generation using period-one nonlinear dynamics of semiconductor lasers

**Kai-Hung Lo,**[1] **Sheng-Kwang Hwang,**[1,2,*] **and Silvano Donati**[3]

[1] *Department of Photonics, National Cheng Kung University, Tainan, Taiwan*
[2] *Advanced Optoelectronic Technology Center, National Cheng Kung University, Tainan, Taiwan*
[3] *Department of Electronics, University of Pavia, Pavia, Italy*
[*] *skhwang@mail.ncku.edu.tw*

**Abstract:** Effects of optical feedback on period-one nonlinear dynamics of an optically injected semiconductor laser are numerically investigated. The optical feedback can suppress the period-one dynamics and excite other more complex dynamics if the feedback level is high except for extremely short feedback delay times. Within the range of the period-one dynamics, however, the optical feedback can stabilize the period-one dynamics in such a manner that significant reduction of microwave linewidth and phase noise is achieved, up to more than two orders of magnitude. A high feedback level and/or a long feedback delay time are generally preferred for such microwave stabilization. However, considerably enhanced microwave linewidth and phase noise happen periodically at certain feedback delay times, which is strongly related to the behavior of locking between the period-one microwave oscillation and the feedback loop modes. The extent of these enhancements reduces if the feedback level is high. While the microwave frequency only slightly changes with the feedback level, it red-shifts with the feedback delay time before an abrupt blue-shift occurs periodically. With the presence of the laser intrinsic noise, frequency jitters occur around the feedback delay times leading to the abrupt blue-shifts, ranging from the order of 0.1 GHz to the order of 1 GHz.



**OCIS codes:** (140.5960) Semiconductor lasers; (140.3520) Lasers, injection-locked; (060.4510) Optical communications; (060.5625) Radio frequency photonics; (350.4010) Microwaves; (190.3100) Instabilities and chaos.

## References and links

1. T. B. Simpson, J. M. Liu, K. F. Huang, and K. Tai, "Nonlinear dynamics induced by external optical injection in semiconductor lasers," Quantum Semiclass. Opt. **9,** 765–784 (1997).
2. S. K. Hwang, J. M. Liu, and J. K. White, "Characteristics of period-one oscillations in semiconductor lasers subject to optical injection," IEEE J. Sel. Top. Quantum Electron. **10,** 974–981 (2004).
3. S. K. Hwang and D. H. Liang, "Effects of linewidth enhancement factor on period-one oscillations of optically injected semiconductor lasers," Appl. Phys. Lett. **89,** 061120 (2006).
4. S. C. Chan, S. K. Hwang, and J. M. Liu, "Period-one oscillation for photonic microwave transmission using an optically injected semiconductor laser," Opt. Express **15,** 14921–14935 (2007).

#214050 - $15.00 USD Received 13 Jun 2014; revised 17 Jul 2014; accepted 17 Jul 2014; published 24 Jul 2014

5. A. Murakami, K. Kawashima, and K. Atsuki, "Cavity resonance shift and bandwidth enhancement in semiconductor lasers with strong light injection," IEEE J. Quantum Electron. **39,** 1196–1204 (2003).
6. S. C. Chan, "Analysis of an optically injected semiconductor laser for microwave generation," IEEE J. Quantum Electron. **46,** 421–428 (2010).
7. S. K. Hwang, S. C. Chan, S. C. Hsieh, and C.Y. Li, "Photonic microwave generation and transmission using direct modulation of stably injection-locked semiconductor lasers," Opt. Commun. **284,** 3581–3589 (2011).
8. S. K. Hwang, H. F. Chen, and C. Y. Lin, "All-optical frequency conversion using nonlinear dynamics of semiconductor lasers," Opt. Lett. **34,** 812–814 (2009).
9. C. H. Chu, S. L. Lin, S. C. Chan, and S. K. Hwang, "All-optical modulation format conversion using nonlinear dynamics of semiconductor lasers," IEEE J. Quantum Electron. **48,** 1389–1396 (2012).
10. S. C. Chan, S. K. Hwang, and J. M. Liu, "Radio-over-fiber AM-to-FM upconversion using an optically injected semiconductor laser," Opt. Lett. **31,** 2254–2256 (2006).
11. Y. H. Hung, C. H. Chu, and S. K. Hwang, "Optical double-sideband modulation to single-sideband modulation conversion using period-one nonlinear dynamics of semiconductor lasers for radio-over-fiber links," Opt. Lett. **38,** 1482–1484 (2013).
12. Y. H. Hung and S. K. Hwang, "Photonic microwave amplification for radio-over-fiber links using period-one nonlinear dynamics of semiconductor lasers," Opt. Lett. **38,** 3355–3358 (2013).
13. T. B. Simpson and F. Doft, "Double-locked laser diode for microwave photonics applications," IEEE Photon. Technol. Lett. **11,** 1476-1478 (1999).
14. S. C. Chan and J. M. Liu, "Tunable narrow-linewidth photonic microwave generation using semiconductor laser dynamics," IEEE J. Sel. Top. Quantum Electron. **10,** 1025–1032 (2004).
15. M. Pochet, N. A. Naderi, Y. Li, V. Kovanis, and L. F. Lester, Tunable photonic oscillators using optically injected quantum-dash diode lasers," IEEE Photon. Technol. Lett. **22,** 763–765 (2010).
16. X. Q. Qi and J. M. Liu, "Photonic microwave applications of the dynamics of semiconductor lasers," IEEE J. Sel. Top. Quantum Electron. **17,** 1198–1211 (2011).
17. Y. S. Yuan and F. Y. Lin, "Photonic generation of broadly tunable microwave signals utilizing a dual-beam optically injected semiconductor laser," IEEE Photon. J. **3,** 644–650 (2011).
18. A. Quirce and A. Valle, "High-frequency microwave signal generation using multi-transverse mode VCSELs subject to two-frequency optical injection," Opt. Express **20,** 13390–13401 (2012).
19. J. P. Zhuang and S. C. Chan, "Tunable photonic microwave generation using optically injected semiconductor laser dynamics with optical feedback stabilization," Opt. Lett. **38,** 344–346 (2013).
20. T. B. Simpson, J. M. Liu, M. AlMulla, N. G. Usechak, and V. Kovanis, "Linewidth sharpening via polarization-rotated feedback in optically-injected semiconductor laser oscillators," IEEE J. Sel. Top. Quantum Electron. **19,** 1500807 (2013).
21. A. Hurtado, J. Mee, M. Nami, I. D. Henning, M. J. Adams, and L. F. Lester, "Tunable microwave signal generator with an optically-injected 1310nm QD-DFB laser," Opt. Express **21,** 10772–10778 (2013).
22. U. Gliese, T. N. Nielsen, M. Bruun, E. L. Christensen, K. E. Stubkjaer, S. Lindgren, and B. Broberg, "A wideband heterodyne optical phase-locked loop for generation of 3–18 GHz Microwave Carriers," IEEE Photon. Technol. Lett. **4,** 936–938 (1992).
23. X. S. Yao and L. Maleki, "Optoelectronic oscillator for photonic systems," IEEE J. Quantum Electron. **32,** 1141–1149 (1996).
24. C. T. Lin, P. T. Shih, W. J. Jiang, J. Chen, P. C. Peng, and S. Chi, "A continuously tunable and filterless optical millimeter-wave generation via frequency octupling," Opt. Express **17,** 19749–19756 (2009).
25. A. Kaszubowska, L. P. Barry, and P. Anandarajah, "Multiple RF carrier distribution in a hybrid radio/fiber system employing a self-pulsating laser diode transmitter," IEEE Photon. Technol. Lett. **14,** 1599–1601 (2002).
26. C. Cui, X. Fu, and S. C. Chan, "Double-locked semiconductor laser for radio-over-fiber uplink transmission," Opt. Lett. **34,** 3821–3823 (2009).
27. V. Annovazzi Lodi, A. Scir, M. Sorel, and S. Donati, "Dynamical behavior and locking of semiconductor laser subjected to injection," IEEE J. Quantum Electron. **34,** 2350–2356 (1998).
28. S. Wieczorek, B. Krauskopf, T. B. Simpson, and D. Lenstra, "The dynamical complexity of optically injected semiconductor lasers," Phys. Rep. **416,** 1–128 (2005).
29. S. Donati and S. K. Hwang, "Chaos and high-level dynamics in coupled lasers and their applications," Prog. Quantum Electron. **36,** 293–341 (2012).
30. T. B. Simpson and J. M. Liu , "Phase and amplitude characteristics of nearly degenerate four-wave mixing in Fabry-Perot semiconductor lasers," J. Appl. Phys. **73,** 2587–2589 (1993).
31. J. M. Liu and T. B. Simpson, "Four-wave mixing and optical modulation in a semiconductor laser," IEEE J. Quantum Electron. **30,** 957–965 (1994).
32. T. B. Simpson and J. M. Liu, "Spontaneous emission, nonlinear optical coupling, and noise in laser diodes," Opt. Commun. **112,** 43–47 (1994).
33. S. K. Hwang, J. B. Gao, and J. M. Liu, "Noise-induced chaos in an optically injected semiconductor laser model," Phys. Rev. E **61,** 5162–5170 (2000).
34. S. K. Hwang, J. M. Liu, and J. K. White, "35-GHz intrinsic bandwidth for direct modulation in 1.3-$\mu$m semicon-

#214050 - $15.00 USD Received 13 Jun 2014; revised 17 Jul 2014; accepted 17 Jul 2014; published 24 Jul 2014

ductor lasers subject to strong injection locking," IEEE Photon. Technol. Lett. **16,** 972–974 (2004).
35. T. B. Simpson and J. M. Liu, "Enhanced modulation bandwidth in injection-locked semiconductor lasers," IEEE Photon. Technol. Lett. **9,** 1322–1324 (1997).
36. T. B. Simpson, J. M. Liu, and A. Gavrielides, "Bandwidth enhancement and broadband noise reduction in injection-locked semiconductor lasers," IEEE Photon. Technol. Lett. **7,** 709–711 (1995).
37. O. Solgaard and K. Y. Lau, "Optical feedback stabilization of the intensity oscillations in ultrahigh-frequency passively modelocked monolithic quantum-well lasers," IEEE Photon. Technol. Lett. **5,** 1264–1266 (1993).
38. C. Y. Lin, F. Grillot, N. A. Naderi, Y. Li, and L. F. Lester, "rf linewidth reduction in a quantum dot passively mode-locked laser subject to external optical feedback," Appl. Phys. Lett. **96,** 051118 (2010).
39. R. Rosales, K. Merghem, A. Martinez, A. Akrout, J. P. Tourrence, A. Accard, F. Lelarge, and A. Ramdane, "InAs/InP quantum-dot passively mode-locked lasers for 1.55-$\mu$ applications," IEEE J. Sel. Top. Quantum Electron. **17,** 1292–1301 (2011).
40. C. Simos, H. Simos, C. Mesaritakis, A. Kapsalis, and D. Syvridis, "Pulse and noise properties of a two section passively mode-locked quantum dot laser under long delay feedback," Opt. Commun. **313,** 248–255 (2014).

## 1. Introduction

By introducing continuous-wave optical injection, period-one (P1) nonlinear dynamics can be excited through undamping the relaxation resonance of semiconductor lasers [1, 2]. The optical intensity of the P1 dynamics undergoes self-sustained oscillation, of which frequency ranges from a few gigahertz to tens or even hundreds of gigahertz [3, 4]. The optical spectrum of the P1 dynamics exhibits a regeneration of the optical injection and oscillation sidebands equally separated from the regeneration by the oscillation frequency. Owing to the red-shifted cavity resonance enhancement [5–7], the lower oscillation sideband is typically much stronger than the upper one. These unique characteristics of the P1 dynamics have attracted increasing research interest for a variety of different optical and microwave signal processing applications.

For example, by taking advantage of the multiple spectral components induced by the optical injection, the P1 dynamics have been proposed for optical frequency conversion [8]. While optical frequency down-, no-, and up-conversion can be simultaneously or individually achieved, the data modulation format, either amplitude modulation (AM), frequency modulation (FM), or phase modulation, can be maintained after conversion. Moreover, since the intensity and frequency of each spectral component depend on the injection level and frequency, the P1 dynamics have also been demonstrated for modulation format conversion between optical AM and optical FM [9] and from optical AM to microwave FM [10]. While different output modulation indices can be achieved by using different spectral components or different injection conditions, simultaneous optical frequency conversion is also possible. In addition, by adopting the intensity asymmetry between the oscillation sidebands, the P1 dynamics have been investigated for conversion from optical double-sideband modulation to optical single-sideband modulation [11]. Self-adaptation to changes in the operating microwave frequency is feasible, and stable operation under fluctuations of the injection level and frequency is achievable. Furthermore, the P1 dynamics have also been studied for photonic microwave amplification [12] by applying the red-shifted cavity resonance enhancement. The amplification can be achieved for a broad microwave range, up to at least 60 GHz, and for a wide gain range, up to at least 30 dB.

In fact, one straightforward, yet promising application of the P1 dynamics is to take advantage of the intensity oscillation excited by the optical injection for photonic microwave generation [13–21]. Broadband frequency tunability, from a few gigahertz to tens or even hundreds of gigahertz, can be achieved by simply adjusting the level and frequency of the optical injection without suffering from limited electronic bandwidths generally encountered in other photonic microwave generation schemes [22–24]. Since the lower oscillation sideband of the P1 dynamics is typically much stronger than the upper one, such generated photonic microwaves possess a characteristic of optical single-sideband modulation and are therefore highly preferred for

#214050 - $15.00 USD Received 13 Jun 2014; revised 17 Jul 2014; accepted 17 Jul 2014; published 24 Jul 2014

fiber distribution to mitigate the microwave power fading effect [4, 25, 26]. However, due to the laser intrinsic noise, the 3-dB linewdith of the photodetected microwaves is typically on the order of tens to hundreds of megahertz, limiting the scope of their practical applications. A few microwave stabilization approaches have therefore been investigated. Simpson et al. demonstrated [13] that the linewidth of the microwaves up to 17 GHz can be reduced below 1 kHz by locking the P1 dynamics to an electronic microwave oscillator operating at the same microwave frequency. To eliminate the need of an electronic microwave oscillator, Chan et al. adopted [14] the optoelectronic feedback of the P1 dynamics as the microwave reference. While a similar reduced linewidth can be achieved for microwaves up to 23 GHz, a photodetector, an electronic microwave amplifier, and an electronic microwave attenuator, which operate at the same microwave frequency, are required in the optoelectronic feedback loop. Since both approaches need electronic microwave components, they become increasingly difficult or/and expensive to implement for increasingly high-frequency microwave applications.

Recently, a microwave stabilization approach based on optical feedback of the P1 dynamics was investigated [19, 20]. The linewidth can be reduced below 50 kHz for microwaves up to 45 GHz. Apparently, the optical feedback approach is much preferred and attractive for high-frequency microwave applications because of its all-optical nature, which bypasses the bandwidth restriction of electronics. However, since the interaction between an external perturbation and a semiconductor laser is highly complex and nonlinear, it is not intuitive and straightforward to expect in advance that an optically injected semiconductor laser at the P1 dynamics would become more stable or more unstable when simultaneously subject to its own optical feedback. Consequently, a deep understanding of the optical feedback effect on the P1 dynamics would help to identify operating conditions leading to the microwave stabilization and to establish design guidelines toward the best possible microwave stabilization. Hence, in this study, we numerically investigate how the optical feedback affects the dynamical and microwave characteristics of the P1 dynamics in semiconductor lasers under various conditions of optical injection and optical feedback. In particular, short to intermediate feedback delay times are emphasized as integrated or small systems are much attractive for practical applications. Following this introduction, the simulation model is presented in Section 2. Results and discussions are reported in Section 3. They are followed by conclusion in Section 4.

## 2. Numerical model

A schematic configuration of a semiconductor laser subject to both optical injection and optical feedback is shown in Fig. 1. The output of a master laser is directed toward a slave laser through an optical circulator. While a variable optical attenuator adjusts the level of the optical injection, a polarization controller aligns the polarization of the optical injection with that of the slave laser. The frequency of the optical injection is varied by tuning either the temperature or the bias current of the master laser. Depending on the level and frequency of the optical injection from the master laser, the slave laser can undergo a variety of different dynamical states [1,27–29], such as stable locking, periodic dynamics, chaos, and four-wave mixing. For our interest in this study, the slave laser is operated under the P1 dynamics for photonic microwave generation. To stabilize the P1 dynamics, part of the slave laser output is fed back through an optical loop. The time and level of the optical feedback are controlled by a variable optical delay line and a variable optical attenuator, respectively. The polarization of the optical feedback is aligned with that of the slave laser through an polarization controller in the feedback loop. The other part of the slave laser output is directed toward a detection system to obtain both optical and microwave spectra.

The laser system can be modeled by the following normalized rate equations of a single-

#214050 - $15.00 USD Received 13 Jun 2014; revised 17 Jul 2014; accepted 17 Jul 2014; published 24 Jul 2014

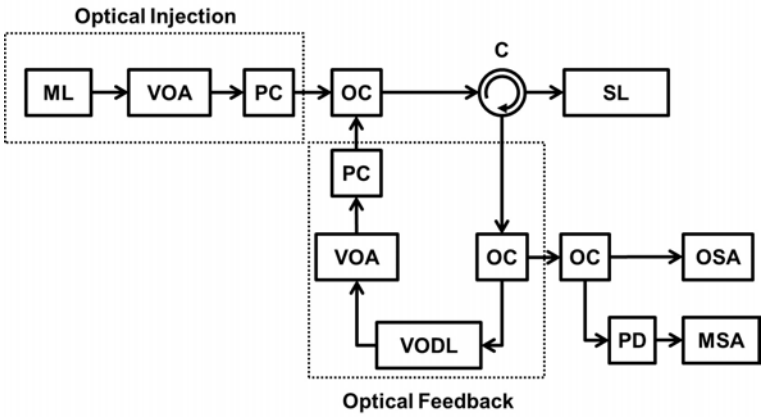


Fig. 1. Schematic of a semiconductor laser subject to optical injection and optical feedback. ML, master laser; VOA, variable optical attenuator; PC, polarization controller; OC, optical coupler; C, optical circulator; SL, slave laser; VODL, variable optical delay line; PD, photodetector; MSA, microwave spectrum analyzer; OSA, optical spectrum analyzer.

mode semiconductor laser subject to both optical injection and optical feedback [30, 31]:

$$\begin{aligned}\frac{da}{dt} &= \frac{1}{2}\left[\frac{\gamma_c\gamma_n}{\gamma_s\tilde{J}}\tilde{n}-\gamma_p(2a+a^2)\right](1+a)+F_a \\ &\quad +\xi_i\gamma_c\cos(\Omega_i t+\phi)+\xi_f\gamma_c[1+a(t-\tau_f)]\cos[\phi(t-\tau_f)-\phi(t)+\theta] \qquad (1)\\ \frac{d\phi}{dt} &= -\frac{b}{2}\left[\frac{\gamma_c\gamma_n}{\gamma_s\tilde{J}}\tilde{n}-\gamma_p(2a+a^2)\right]+\frac{F_\phi}{1+a} \\ &\quad -\frac{\xi_i\gamma_c}{1+a}\sin(\Omega_i t+\phi)+\xi_f\gamma_c\frac{1+a(t-\tau_f)}{1+a(t)}\sin[\phi(t-\tau_f)-\phi(t)+\theta] \qquad (2)\\ \frac{d\tilde{n}}{dt} &= -\gamma_s\tilde{n}-\gamma_n(1+a)^2\tilde{n}-\gamma_s\tilde{J}(2a+a^2)+\frac{\gamma_s\gamma_p}{\gamma_c}\tilde{J}(2a+a^2)(1+a)^2 \qquad (3)\end{aligned}$$

Here, $a$ and $\tilde{n}$ are the normalized field amplitude and carrier density of the slave laser, respectively, while $\phi$ is the phase difference between the injection field and the slave laser. Laser intrinsic parameters, $\gamma_c, \gamma_s, \gamma_n, \gamma_p$, and $b$ are the cavity decay rate, spontaneous carrier relaxation rate, differential carrier relaxation rate, nonlinear carrier relaxation rate, and linewidth enhancement factor, respectively. The normalized Langevin noise-source parameters $F_a$ and $F_\phi$ are characterized by a spontaneous emission rate $R_{sp}$ [32, 33]. The normalized bias current, $\tilde{J}$, represents the bias level above the threshold of the slave laser. The normalized injection parameter, $\xi_i$, is proportional to the ratio of the optical fields between the optical injection signal and the free-running slave laser, the square of which is proportional to the injection power actually received by the slave laser. The detuning frequency, $f_i = \Omega_i/2\pi$, is the frequency offset of the injection from the free-running frequency of the slave laser. The normalized feedback parameter, $\xi_f$, measures the strength of the optical feedback signal. The feedback delay time, $\tau_f$, is the time required for the optical feedback signal travelling back to the slave laser. The phase factor, $\theta$, is the phase difference between the feedback field and the intracavity field at the feedback injection point. To simplify our study, $\theta$ is set equal to zero throughout the numerical calculation.

The values of the intrinsic parameters adopted in this study are $\gamma_c = 5.36\times10^{11}$ s$^{-1}$, $\gamma_s = 5.96\times10^{9}$ s$^{-1}$, $\gamma_p = 1.91\times10^{10}$ s$^{-1}$, $\gamma_n = 7.53\times10^{9}$ s$^{-1}$, and $b = 3$. These values were

#214050 - $15.00 USD Received 13 Jun 2014; revised 17 Jul 2014; accepted 17 Jul 2014; published 24 Jul 2014

experimentally determined in our previous work [34] where the laser was biased at 40 mA, corresponding to $\tilde{J} = 1.222$, with an output power of 4.5 mW. The relaxation resonance frequency of the free-running slave laser is given by $f_r = (2\pi)^{-1}(\gamma_c\gamma_n + \gamma_s\gamma_p)^{1/2} \approx 10.25$ GHz. The spontaneous emission rate is taken to be $R_{sp} = 4.7 \times 10^{19}$ $V^2m^{-1}s^{-1}$. A second-order Runge-Kutta method with the measured laser parameters is used to solve Eqs. (1)–(3), which has been demonstrated to reproduce all the experimentally observed phenomena in such a laser system [1, 2]. The time durations of one integration step and one complete integration adopted in this study are about 0.95 ps and 0.51 ms, respectively, the latter of which gives rise to a frequency resolution of about 2 kHz. The validity of the numerical model described above has been verified with experimental data for the operating conditions considered in this study [2, 4, 7, 34, 35].

## 3. Results and analyses

### *3.1. Dynamical characteristics*

To investigate the optical feedback effect on the P1 dynamics, representative optical and microwave spectra of the slave laser subject to both optical injection at $(\xi_i, f_i) = (0.4, 40$ GHz) and optical feedback at different $(\xi_f, \tau_f)$ are shown in Fig. 2. To identify the resulting dynamical states when the optical feedback is introduced, their inherent dynamical characteristics are analyzed through the spectra where the laser intrinsic noise is not considered in the numerical calculation, shown as the red curves in Fig. 2. To study the linewidth and phase noise of the resulting microwaves when the optical feedback is introduced, the spectra which take the laser intrinsic noise into account in the numerical calculation are presented as the gray curves in Fig. 2.

First consider the optical spectra of the slave laser subject to optical injection only, as shown in Fig. 2(a-i), where a P1 dynamical state is excited. While a regeneration of the optical injection appears at the offset frequency of 40 GHz because of the injection pulling effect [29], oscillation sidebands equally separated from the regeneration by an oscillation frequency $f_0 = 46.06$ GHz emerge through undamping the laser relaxation resonance. Since the optical injection reduces the necessary gain for the slave laser, the laser cavity resonance red-shifts through the antiguidance effect [6]. Accordingly, the lower oscillation sideband is resonantly enhanced as opposed to the upper one, resulting in a characteristic of optical single-sideband modulation. Except the broadening around each spectral component and the appearance of the noise pedestal, these key features of the P1 dynamical state are similarly observed when the laser noise is considered. Figure 2(a-ii) shows the resulting microwave spectra of the P1 dynamical state after photodetection, where a microwave signal at $f_0 = 46.06$ GHz is observed. The 3-dB linewidth, $\Delta\nu$, of the microwave signal broadens considerably from about 2 kHz, which should be 0 Hz theoretically but is limited numerically by the frequency resolution of our computing capability, to 90.7 MHz when the laser noise is considered. Note that, in this study, the microwave linewidth is estimated by measuring the 3-dB linewidth of the Lorentzian fitting curve of each microwave spectrum.

Similar P1 dynamical states are identified for a variety of different optical injection conditions, which dominate the dynamical mapping of the optically injected laser above the Hopf bifurcation line separating the P1 dynamics from the stable locking dynamics [1–4,6]. The dynamical mapping based upon the same values of the laser intrinsic parameters considered in this study can be found in our previous works [3, 4]. The feasibility of exciting various P1 dynamical states over a broad range of the optical injection condition provides a possibility to dynamically reconfigure the same laser system for different operating requirements in practical applications. Indeed, even though different P1 dynamical states exhibit qualitatively similar spectral features addressed above, there exist quantitative differences [1–4,6,11]. For example,

#214050 - $15.00 USD Received 13 Jun 2014; revised 17 Jul 2014; accepted 17 Jul 2014; published 24 Jul 2014

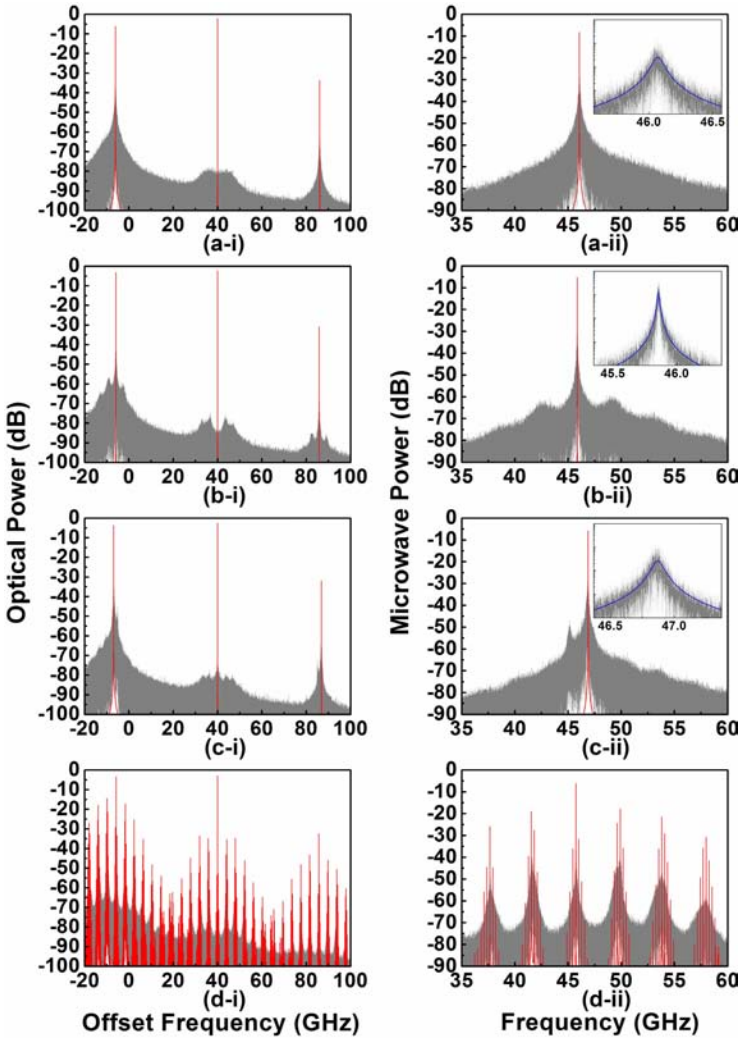


Fig. 2. Optical spectra (left column) and microwave spectra (right column) of the slave laser subject to both optical injection at $(\xi_i, f_i) = (0.4, 40\ \text{GHz})$ and optical feedback at $(\xi_f, \tau_f) = (0, 0\ \text{ns})$ for (a-i)(a-ii), $(0.005, 0.21\ \text{ns})$ for (b-i)(b-ii), $(0.005, 0.28\ \text{ns})$ for (c-i)(c-ii), and $(0.027, 0.21\ \text{ns})$ for (d-i)(d-ii), respectively. Red curves, no laser noise is considered; Gray curves, laser noise is considered. The $x$ axes of the optical spectra are relative to the free-running frequency of the slave laser. The figure shown in each inset is an enlargement of each corresponding microwave spectrum in a linear scale with a Lorentzian fitting curve (blue curve).

$f_0$ can be enhanced by increasing $\xi_i$ or/and $f_i$, giving rise to a broadly and continuously tunable $f_0$ from 10 GHz up to 65 GHz for the operating conditions under consideration [2–4,6]. An even higher $f_0$ can be obtained, such as 100 GHz, if $\xi_i$ or $f_i$ is further increased [10], if a higher $f_r$ is given to begin with by using a higher bias level of the same laser [36] or a different laser with higher speed [34, 35], or if a larger $b$ value is possible [3].

By optically sending a small fraction of the optical signal shown in Fig. 2(a-i) back to the slave laser at $(\xi_f, \tau_f) = (0.005, 0.21\ \text{ns})$, the key P1 features are mostly preserved no matter

#214050 - $15.00 USD Received 13 Jun 2014; revised 17 Jul 2014; accepted 17 Jul 2014; published 24 Jul 2014

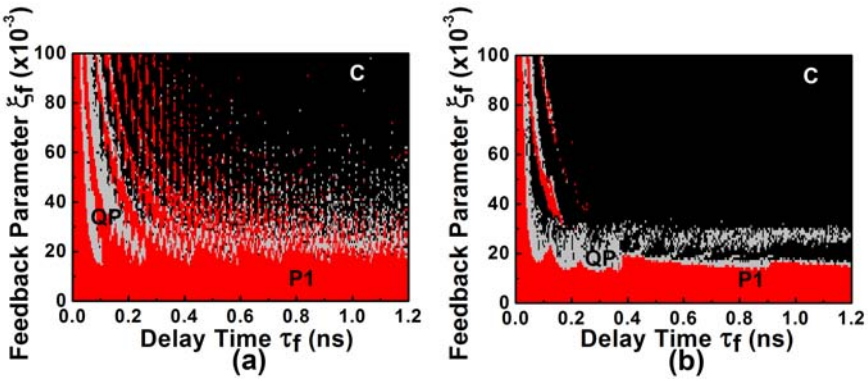


Fig. 3. Dynamical mappings of the slave laser subject to both optical injection and optical feedback in terms of $\xi_{\mathrm{f}}$ and $\tau_{\mathrm{f}}$ at (a) $(\xi_{\mathrm{i}}, f_{\mathrm{i}}) = (0.4, 40\ \mathrm{GHz})$ and (b) $(\xi_{\mathrm{i}}, f_{\mathrm{i}}) = (0.2, 40\ \mathrm{GHz})$, respectively. P1, period-one dynamics; QP, quasi-periodic dynamics; C, chaos and other instabilities.

whether the laser noise is considered or not, as presented in Fig. 2(b-i). Therefore, the resulting dynamical state is intrinsically a P1 state. Since forming a feedback loop gives rise to an extra resonance condition for the laser system to satisfy, there exist modifications in the P1 characteristics after the introduction of the optical feedback. First, while the regeneration still appears at 40 GHz offset frequency, the oscillation sidebands actually shift toward the regeneration by about 0.21 GHz, resulting in a reduced $f_0 = 45.85$ GHz. Second, side peaks equally separated by about 3.3 GHz from each P1 spectral component appear when the laser noise is present. This frequency separation is close to the feedback loop frequency $f_l = 4.88$ GHz determined by the reciprocal of the feedback delay time $\tau_{\mathrm{f}}$ under study. As $\xi_{\mathrm{f}}$ or $\tau_{\mathrm{f}}$ increases, the intensity of the side peaks enhances. In addition, the frequency separation between the side peaks approaches $f_l$ and finally matches with $f_l$ when $\xi_{\mathrm{f}}$ or $\tau_{\mathrm{f}}$ is considerably large. This observation suggests that the emerging side peaks are actually the resonance modes formed by the optical feedback loop, which are modified to some extent depending on the conditions of both optical injection and optical feedback. These modifications of the P1 characteristics can be more easily identified in Fig. 2(b-ii), where a red-shifted microwave signal at $f_0 = 45.85$ GHz is observed and is surrounded by side peaks with a frequency separation of about 3.3 GHz. In addition, the microwave linewidth $\Delta\nu$ is found to reduce down to 19.2 MHz from 90.7 MHz shown in Fig. 2(a-ii).

Globally similar, yet locally different characteristic modifications of the P1 dynamical state are observed for a variety of different optical feedback conditions. As shown in Figs. 2(c-i) and 2(c-ii) where $(\xi_{\mathrm{f}}, \tau_{\mathrm{f}}) = (0.005, 0.28\ \mathrm{ns})$, for example, not only $f_0$ increases to 46.9 GHz but also $\Delta\nu$ broadens to 91.8 MHz, broader than the one when no optical feedback is introduced in Fig. 2(a-ii). Detailed studies on the variations of these microwave characteristics under different $(\xi_{\mathrm{f}}, \tau_{\mathrm{f}})$ will be demonstrated in the next section. On the other hand, the introduction of the optical feedback can also suppress the P1 dynamical state and excite others, such as quasi-periodicity and chaos, under various different feedback conditions. For example, Figs. 2(d-i) and 2(d-ii) show a quasi-periodic state when $(\xi_{\mathrm{f}}, \tau_{\mathrm{f}}) = (0.027, 0.21\ \mathrm{ns})$. The laser noise more or less smears out the fine structure of the quasi-periodicity, which may make it difficult to be identified experimentally. Figure 3(a) summarizes the observed dynamical states as a function of $(\xi_{\mathrm{f}}, \tau_{\mathrm{f}})$ under consideration, which are mainly dominated by the P1, quasi-periodic, and chaotic dynamics. A continuous distribution of the P1 dynamics is found when $\xi_{\mathrm{f}} \leq 0.015$ or $\tau_{\mathrm{f}} \leq 33.3$ ps under study. While a similar structure of the dynamical mapping is observed,

#214050 - $15.00 USD Received 13 Jun 2014; revised 17 Jul 2014; accepted 17 Jul 2014; published 24 Jul 2014

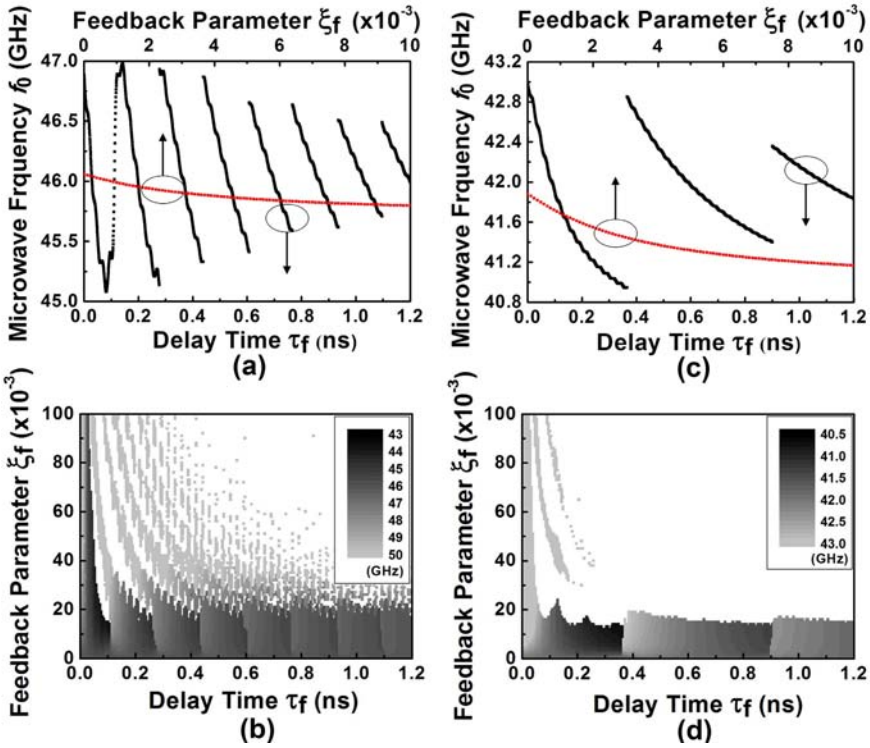


Fig. 4. (a)(c) Microwave frequency $f_0$ in terms of $\xi_f$ at $\tau_f = 0.21$ ns and in terms of $\tau_f$ at $\xi_f = 0.005$. (b)(d) Mappings of microwave frequency $f_0$ in terms of $\xi_f$ and $\tau_f$. Left column, $(\xi_i, f_i) = (0.4, 40$ GHz); Right column, $(\xi_i, f_i) = (0.2, 40$ GHz).

the distribution of the P1 dynamics is compressed by the spread of the others if the optical injection condition leading to the P1 dynamics is chosen away from the Hopf bifurcation line. An example of such a dynamical mapping is demonstrated in Fig. 3(b) where $(\xi_i, f_i) = (0.2,$ 40 GHz).

### *3.2. Microwave characteristics*

As pointed out in the previous discussion, different microwave characteristics of the P1 dynamics are observed under different optical feedback conditions. Let us first study how the microwave frequency actually changes with the optical feedback, as demonstrated in Figs. 4 to 6. Note that the laser noise is not considered in the numerical calculation in Figs. 4 to 6 in order to investigate the intrinsic variation of the microwave frequency. In Fig. 4(a) where $(\xi_i, f_i)$ $= (0.4,$ 40 GHz), $f_0$ is observed to red-shift continuously with $\tau_f$, in general, but blue-shift abruptly at certain $\tau_f$ values. Since forming a feedback loop leads to an additional resonance condition for the laser system to satisfy, this behavior of $f_0$ reveals the fact that the intensity oscillation of the P1 dynamics can stably appear only at frequencies that are integral multiples of the feedback loop frequency $f_l$. That is, when the optical feedback is introduced, the intensity oscillation of the P1 dynamics locks on to the closest mode of the optical feedback loop. Progressive enhancement of $\tau_f$ results in the progressive red-shift of all feedback loop modes. This in turn leads to the progressive red-shift of $f_0$ until $\tau_f$ reaches a value when two feedback loop modes appear approximately equally from the intensity oscillation of the intrinsic P1 dynamics without optical feedback. A slight further enhancement of $\tau_f$ would lock the P1 dynamics to the

#214050 - $15.00 USD Received 13 Jun 2014; revised 17 Jul 2014; accepted 17 Jul 2014; published 24 Jul 2014

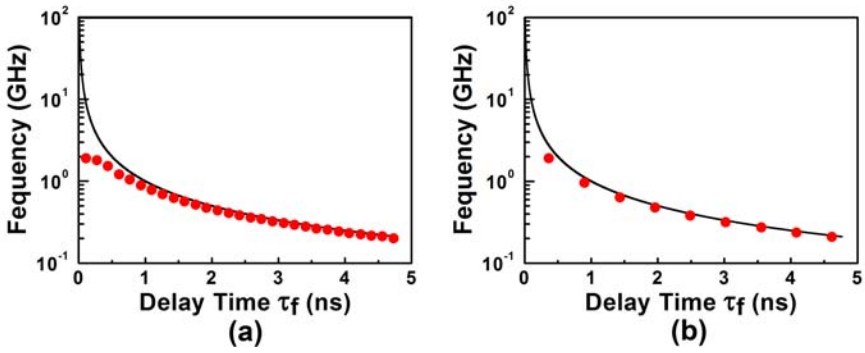


Fig. 5. Microwave frequency blue-shift $\Delta f_0$ (red circles) and feedback loop frequency $f_l$ (black curves) in terms of $\tau_f$ at $\xi_f$ =0.005 for (a) $(\xi_i, f_i) = (0.4, 40\ \text{GHz})$ and (b) $(\xi_i, f_i) = (0.2, 40\ \text{GHz})$, respectively.

feedback loop mode at a higher frequency, giving rise to an abrupt blue-shift of $f_0$, $\Delta f_0$, equal to the frequency separation between the two feedback loop modes. The same process repeats with a period of $T_1 = 164.4$ ps in Fig. 4(a). A similar saw-type behavior of $f_0$ has been observed as well in mode-locked semiconductor lasers subject to optical feedback [37–40]. Since the frequency separation between the feedback loop modes is mainly determined by $f_l$, $\Delta f_0$ is expected and is indeed observed in Fig. 4(a) to reduce with $\tau_f$. In addition, $\Delta f_0$ is also expected to behave the same as $f_l$ does when $\tau_f$ enhances, as demonstrated in Fig 5(a), where it deviates from $f_l$ at small $\tau_f$ values but approaches $f_l$ as $\tau_f$ increases. This result also supports the previous discussion that the frequency separation between the feedback loop modes approaches $f_l$ as $\tau_f$ increases and finally matches with $f_l$ when $\tau_f$ is considerably large.

The same $\tau_f$ dependence of $f_0$ applies to other $\xi_f$ values. This can be verified by analyzing $f_0$ in terms of $\xi_f$, as also shown in Fig. 4(a), where $f_0$ changes slightly and monotonically. For a more complete understanding, the dependence of $f_0$ on both $\xi_f$ and $\tau_f$ is presented as a mapping in Fig. 4(b). A periodic variation of $f_0$ as a function of $\tau_f$ with a constant $T_1 = 164.4$ ps is clearly observed for $\xi_f \leq 0.015$. The dependence of $f_0$ on both $\xi_f$ and $\tau_f$, however, becomes more complicated for $\xi_f > 0.015$ where dynamical states other than the P1 dynamics are excited. Qualitatively similar behaviors of $f_0$ as a function of $(\xi_f, \tau_f)$ are also observed for other optical injection conditions. An example is presented in Figs. 4(c) and 4(d) for $(\xi_i, f_i) = (0.2, 40\ \text{GHz})$. A closely similar behavior of $\Delta f_0$ in terms of $\tau_f$ is expected since $\Delta f_0$ depends mainly on $f_l$, the reciprocal of $\tau_f$. This is indeed observed in Figs. 4(c) and 4(d) and is further verified in Fig. 5(b). On the other hand, a longer period of $T_1 = 534.54$ ps is observed in Figs. 4(c) and 4(d), suggesting that it depends strongly on $(\xi_i, f_i)$. The study of mode-locked semiconductor lasers subject to optical feedback found that $T_1$ is equal to the reciprocal of the pulse repetition rate, or equivalently $f_0$, in such laser systems [37–40]. However, as demonstrated in Fig. 6(a) for various different $(\xi_i, f_i)$, $T_1$ in the present laser system is not equal to the reciprocal of $f_0$ but the reciprocal of the frequency difference between the lower oscillation sideband of the intrinsic P1 dynamics without optical feedback and the free-running slave laser. Based on the study of the P1 dynamics in optically injected semiconductor lasers [2, 3], the lower oscillation sideband blue-shifts toward the free-running frequency of the slave laser as $\xi_i$ reduces or $f_i$ increases. Therefore, a smaller $\xi_i$ or a larger $f_i$ results in a longer period of $T_1$, as observed in Figs. 4(c) and 4(d). This in turn leads to slower red-shifts and less frequent blue-shifts of $f_0$ as a function of $\tau_f$, making $f_0$ less sensitive to the change in $\tau_f$ because of possible ambiance variation. Since different combinations of $(\xi_i, f_i)$ can lead to a same $f_0$ [2–4,6,11], it is feasible

#214050 - $15.00 USD Received 13 Jun 2014; revised 17 Jul 2014; accepted 17 Jul 2014; published 24 Jul 2014

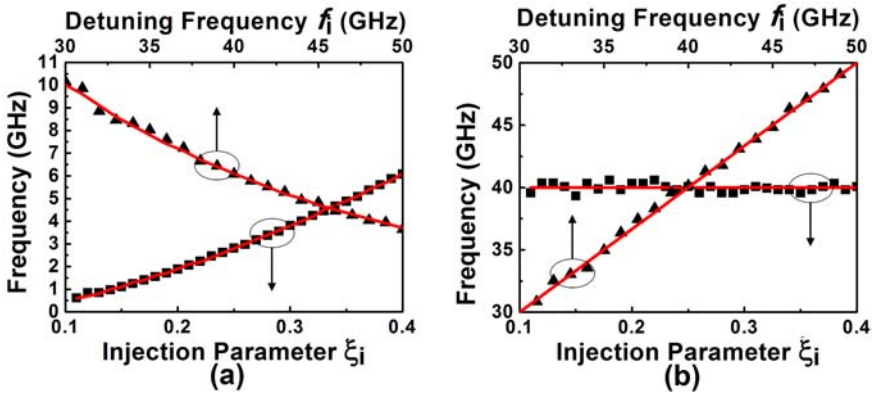


Fig. 6. (a) Reciprocal of $T_1$ (black triangles and squares) and frequency difference between the lower P1 oscillation sideband and the free-running slave laser (red curves) in terms of $\xi_i$ at $f_i = 40$ GHz and in terms of $f_i$ at $\xi_i = 0.4$. (b) Reciprocal of $T_2$ (black triangles and squares) and frequency difference between the optical injection signal and the free-running slave laser (red curves) in terms of $\xi_i$ at $f_i = 40$ GHz and in terms of $f_i$ at $\xi_i = 0.4$.

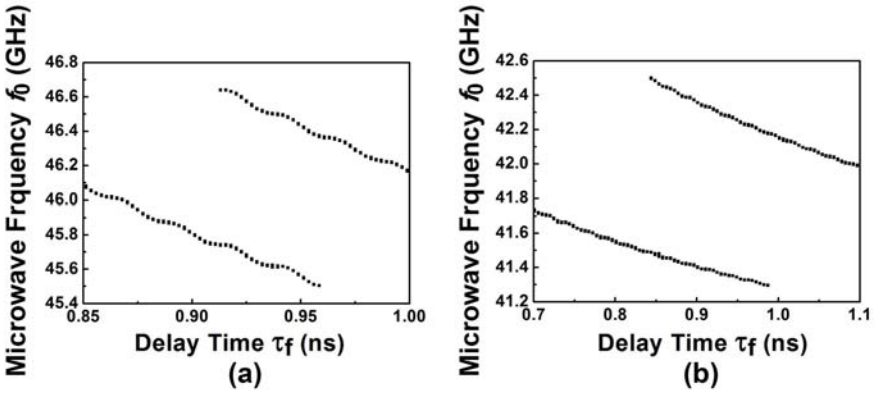


Fig. 7. (a)(b) Enlargement of Figs. 4(a) and 4(c), respectively, for microwave frequency $f_0$ in terms of $\tau_f$ at $\xi_f = 0.005$ when the laser noise is considered.

to choose one such combination with a long $T_1$ so that $f_0$ is relatively stable.

Before proceeding to the analysis of how the microwave phase quality actually changes with the optical feedback, two more characteristics of the microwave frequency as a function of $\tau_f$ are addressed here. First, by closely looking into Fig. 4(a) and 4(c), continuous ripples of $f_0$ are observed with a period of $T_2 = 24.99$ and 24.89 ps, respectively, while it red-shifts with $\tau_f$ between abrupt blue-shifts. This periodicity, as demonstrated in Fig. 6(b), is equal to the reciprocal of the frequency difference between the optical injection signal and the free-running slave laser, i.e., $f_i$. Second, as previously discussed, an abrupt blue-shift occurs if $\tau_f$ enhances slightly beyond a specific value when two feedback loop modes appear approximately equally from the intensity oscillation of the intrinsic P1 dynamics. This implies that, if the laser noise is taken into account in the numerical calculation in Figs. 4(a) and 4(c), such an abrupt blue-shift could occur not only at that specific $\tau_f$ value but also over a limited range of $\tau_f$ around it. Indeed, as shown in Figs. 7(a) and 7(b) where not only the laser noise is taken into account in the numerical calculation but also multiple independent noise realizations are conducted, two $f_0$

#214050 - $15.00 USD Received 13 Jun 2014; revised 17 Jul 2014; accepted 17 Jul 2014; published 24 Jul 2014

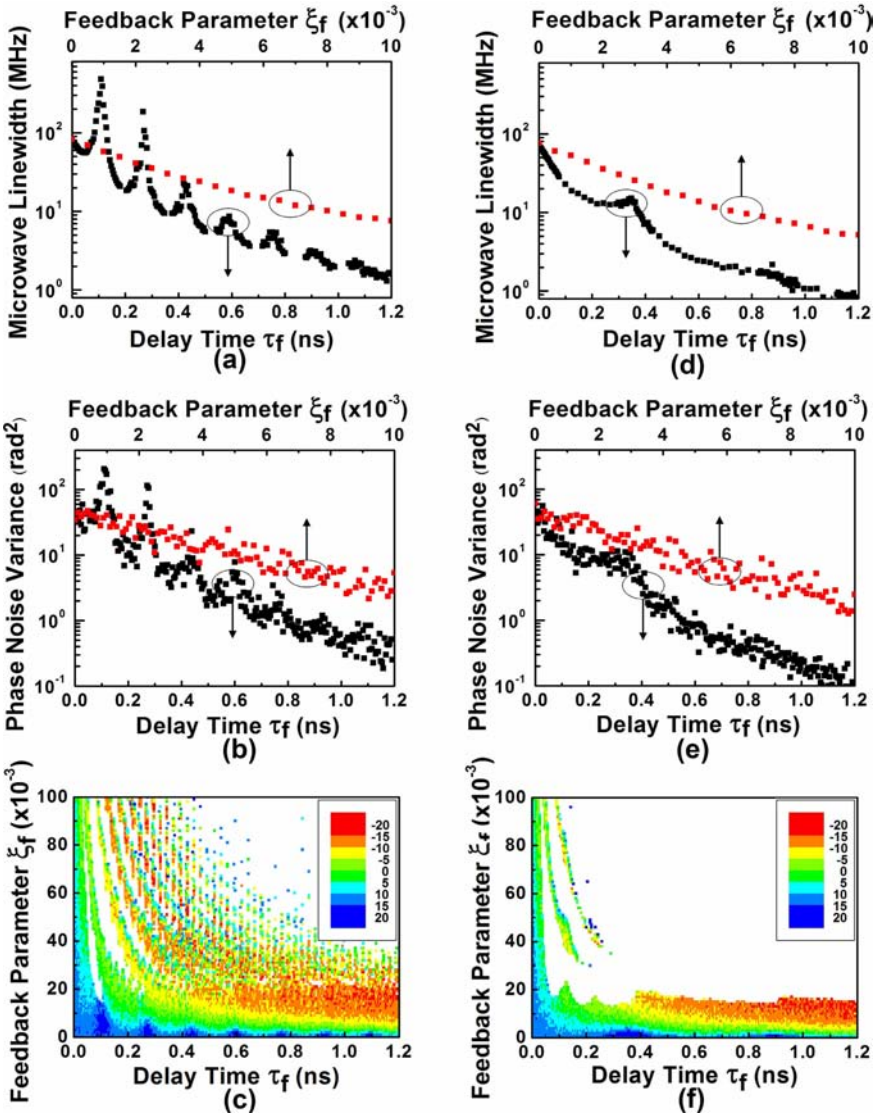


Fig. 8. (a)(d) Microwave linewdith $\Delta\nu$ and (b)(f) phase noise variance in terms of $\xi_f$ at $\tau_f = 0.21$ ns and in terms of $\tau_f$ at $\xi_f$ =0.005. (c)(g) Mappings of phase noise variance in terms of $\xi_f$ and $\tau_f$, where its log-scaled values are presented. Left column, $(\xi_i, f_i) = (0.4,$ 40 GHz); Right column, $(\xi_i, f_i) = (0.2, 40$ GHz).

values are found possible for each $\tau_f$ over a limited range. This suggests that, when the optical feedback is introduced at certain $\tau_f$ values, the resulting microwaves would practically suffer from frequency jitters, which range from the order of 1 GHz down to the order of 0.1 GHz for the operating conditions under study.

Let us next turn our attention to the investigation of the microwave phase quality, namely linewidth and phase noise, when the optical feedback is introduced, as presented in Fig. 8. Note that the laser intrinsic noise is considered in the numerical calculation here in order to conduct the analysis of these microwave characteristics. Figure 8(a) shows the 3-dB microwave

#214050 - $15.00 USD Received 13 Jun 2014; revised 17 Jul 2014; accepted 17 Jul 2014; published 24 Jul 2014

linewidth $\Delta\nu$ as a function of $(\xi_f, \tau_f)$ when $(\xi_i, f_i) = (0.4, 40\ \text{GHz})$. First, $\Delta\nu$ reduces with $\xi_f$ as a higher level of the optical feedback signal locks the P1 dynamics more strongly. Second, from a macroscopic viewpoint, $\Delta\nu$ decreases with $\tau_f$ as a longer delay of the optical feedback signal loses more its coherence with the intracavity optical field of the slave laser. From a microscopic viewpoint, however, $\Delta\nu$ increases considerably at certain $\tau_f$ values, making the microwave linewidth possible to become much broader than the one before the optical feedback is introduced. By comparing Fig. 8(a) with Fig. 4(a), such a considerable enhancement of $\Delta\nu$ is found to happen when an abrupt blue-shift of $f_0$ occurs. In addition, a local minimum of $\Delta\nu$ is observed between two such $\Delta\nu$ enhancements and is found to happen around the midway of each $f_0$ red-shift with $\tau_f$. As addressed above, when the optical feedback is introduced, the intensity oscillation of the P1 dynamics locks on to the closest mode of the optical feedback loop. The behavior of $\Delta\nu$ as a function of $\tau_f$ therefore suggests that $\Delta\nu$ reduces to a local minimum when this feedback loop mode oscillates exactly at $f_0$ of the intrinsic P1 dynamics without optical feedback. When this feedback loop mode red-shifts away as $\tau_f$ enhances, $\Delta\nu$ starts to broaden, a local maximum of which is reached when two feedback loop modes appear approximately equally from the intensity oscillation of the intrinsic P1 dynamics. This process repeats with the same period of $T_l = 164.4$ ps as in Fig. 4(a). Similar behaviors of $\Delta\nu$ as a function of $(\xi_f, \tau_f)$ are also observed for other optical injection conditions, such as the ones shown in Fig. 8(d) where $(\xi_i, f_i) = (0.2, 40\ \text{GHz})$ and $T_l = 534.54$ ps. If $(\xi_i, f_i)$ leading to the P1 dynamics is chosen away from the Hopf bifurcation line, not only the extent of the considerable enhancements in $\Delta\nu$ reduces but also the period of these enhancements increases, suggesting that the reduced $\Delta\nu$ are less sensitive to the change in $\tau_f$.

The microwave phase quality is further investigated through analyzing the single-sideband phase noise of the resulting microwaves after the optical feedback is introduced. To quantify the phase noise over a broad range, the phase noise variance is estimated by integrating the single-sideband phase noise from the frequency offset of 1 MHz to 500 MHz [19]. For the range of $\tau_f$ under study, this integration does not include feedback loop modes, thus eliminating the contribution of the phase noise from the modes. As shown in Fig. 8(b) where $(\xi_i, f_i) = (0.4, 40\ \text{GHz})$, the behavior of the phase noise variance as a function of $(\xi_f, \tau_f)$ agrees well with that of the microwave linewidth shown in Fig. 8(a). The dependence of the phase noise variance on both $\xi_f$ and $\tau_f$ is also presented as a mapping in Fig. 8(c). A periodic variation of the phase noise variance as a function of $\tau_f$ with a constant $T_l = 164.4$ ps is clearly observed at small $\xi_f$ values. However, as opposed to the periodic variation of the microwave frequency shown in Fig. 4(b), this periodic variation of the phase noise variance becomes less significant as $\xi_f$ increases. This is due to the fact that the effect of $\xi_f$ on the phase noise is much stronger than that on the microwave frequency, as clearly demonstrated in Figs. 4(a) and 8(b). The dependence of the phase noise variance on both $\xi_f$ and $\tau_f$ become more complicated for $\xi_f > 0.015$ where dynamical states other than the P1 dynamics are excited. Similar behaviors of the phase noise variance as a function of $(\xi_f, \tau_f)$ are also observed for other optical injection conditions, such as the ones shown in Figs. 8(e) and 8(f) where $(\xi_i, f_i) = (0.2, 40\ \text{GHz})$. If $(\xi_i, f_i)$ leading to the P1 dynamics is chosen away from the Hopf bifurcation line, not only the extent of the considerable enhancements in phase noise variance reduces but also the period of these enhancements increases, suggesting that the reduced phase noise varinace are less sensitive to the change in $\tau_f$.

## 4. Conclusion

Effects of optical feedback on P1 nonlinear dynamics of an optically injected semiconductor laser are numerically investigated by analyzing their dynamical and microwave characteristics under various operating conditions. The optical feedback can suppress the P1 dynamics and

#214050 - $15.00 USD Received 13 Jun 2014; revised 17 Jul 2014; accepted 17 Jul 2014; published 24 Jul 2014

excite other more complex dynamics if the feedback level is high except for extremely short feedback delay times. The region of the P1 dynamics as a function of the optical feedback condition shrinks if the optical injection condition is chosen away from the Hopf bifurcation line to begin with. Within the region of the P1 dynamics, the optical feedback can stabilize the P1 dynamics in such a manner that significant reduction of microwave linewidth and phase noise is achieved, up to more than two orders of magnitude for the range of operating conditions under study. Such considerably improved microwave phase quality is important to optically generate stabilized microwaves through the P1 dynamics schemes. Generally speaking, a high feedback level and/or a long feedback delay time are preferred to achieve the best possible microwave stabilization. However, considerably enhanced microwave linewidth and phase noise happen periodically at certain feedback delay times. The underlying mechanism of these enhancements is strongly related to the behavior of locking between the intensity oscillation of the intrinsic P1 dynamics without optical feedback and the resonance modes of the optical feedback loop. The periodicity is equal to the reciprocal of the frequency difference between the lower oscillation sideband of the intrinsic P1 dynamics and the free-running slave laser. The extent of these enhancements reduces if the feedback level is high. If the optical injection condition is chosen away from the Hopf bifurcation line to begin with, not only the extent of these enhancements reduces but also the periodicity of these enhancements increases, suggesting that the reduced microwave linewidth and phase noise are less sensitive to the change in the feedback delay time. While the microwave frequency only slightly changes with the feedback level, it red-shifts with the feedback delay time before an abrupt blue-shift occurs with the same periodicity observed in the microwave linewdith and phase noise. The amount of the abrupt blue-shift equals the frequency separation between the feedback loop modes and therefore decreases with the feedback delay time. With the presence of the laser intrinsic noise, frequency jitters occur around the feedback delay times leading to the abrupt blue-shifts, ranging from the order of 0.1 GHz to the order of 1 GHz for the range of operating conditions under study. If the optical injection condition is chosen away from the Hopf bifurcation line to begin with, slower red-shifts and less frequent blue-shifts of the microwave frequency as a function of the feedback delay time are obtained, making the microwave frequency less sensitive to the change in the feedback delay time. Since different combinations of the optical injection condition can lead to one same microwave frequency, it is feasible to choose one combination such that the microwave frequency is relatively stable.

**Acknowledgments**

S.K. Hwang's work is supported by the National Science Council of Taiwan under Contract NSC102-2112-M-006-004.

#214050 - $15.00 USD Received 13 Jun 2014; revised 17 Jul 2014; accepted 17 Jul 2014; published 24 Jul 2014